Augmented Reality-based Contextual Guidance through Surgical Tool Tracking in Neurosurgery

Sangjun Eom, *Graduate Student Member, IEEE*, Seijung Kim, *Student Member, IEEE*, Joshua Jackson, David Sykes, Shervin Rahimpour, and Maria Gorlatova, *Member, IEEE*

Abstract—External ventricular drain (EVD) is a common, yet challenging neurosurgical procedure of placing a catheter into the brain ventricular system that requires prolonged training for surgeons to improve the catheter placement accuracy. In this paper, we introduce NeuroLens, an Augmented Reality (AR) system that provides neurosurgeons with guidance that aids them in completing an EVD catheter placement. NeuroLens builds on prior work in AR-assisted EVD to present a registered hologram of a patient's ventricles to the surgeons, and uniquely incorporates guidance on the EVD catheter's trajectory, angle of insertion, and distance to the target. The guidance is enabled by tracking the EVD catheter. We evaluate NeuroLens via a study with 33 medical students and 9 neurosurgeons, in which we analyzed participants' EVD catheter insertion accuracy and completion time, eye gaze patterns, and qualitative responses. Our study, in which NeuroLens was used to aid students and surgeons in inserting an EVD catheter into a realistic phantom model of a human head, demonstrated the potential of NeuroLens as a tool that will aid and educate novice neurosurgeons. On average, the use of NeuroLens improved the EVD placement accuracy of the year 1 students by 39.4%, of the year 2−4 students by 45.7%, and of the neurosurgeons by 16.7%. Furthermore, students who focused more on NeuroLens-provided contextual guidance achieved better results, and novice surgeons improved more than the expert surgeons with NeuroLens's assistance.

Index Terms—Augmented reality, neurosurgery, contextual guidance, tool tracking, image registration.

1 Introduction

The external ventricular drain (EVD) is a common neurosurgical procedure for patients with hydrocephalus, meningitis, and traumatic injury [38]. In EVD, the cerebrospinal fluid is drained to relieve pressure buildup within the skull by placing a catheter into the brain ventricular system via a small opening in the skull. Despite being practiced more than 20,000 times annually in the U.S. [41], the challenges of the EVD procedure come from relying on the surgeon's expertise and the external anatomical landmarks of the patients to estimate the target. A standard EVD catheter placement is performed at the bedside without any aides ('freehand') under emergency conditions. Other aides such as a neuronavigation system or computed tomography (CT) scan are used for special cases of the patients such as having an intraventricular hemorrhage or a midline shift that results in an asymmetrical brain ventricle. The success rate of the freehand EVD is around 73% [53]; this rate is lower for less experienced surgeons [43]. A misplacement of the EVD can lead to serious complications such as ventriculitis, brain abscesses, or subdural empyema [17]. Thus, prolonged training [40] or guidance of CT scan [2] is required to improve the catheter placement accuracy of this 'freehand' approach.

Due to these challenges, EVD is a prime example of a neurosurgical procedure that can benefit from the integration of Augmented Reality (AR), guiding surgeons in a more convenient and intuitive manner [7]. The anatomical visualization in AR substantially enhances the surgeon's perception of the surgical environment [37] and increases confidence regarding precision [22] during the procedure, where the surgeon's field of view (FoV) is often limited. To provide guidance to surgeons via anatomical visualization, marker-based image registration has been adopted in several lines of work that integrated AR with EVD [31], [47], [58]. In these systems, a 3D hologram of the patient's ventricles is rendered in the corresponding location within the skull, allowing surgeons to see the area they are targeting. Though anatomical visualization enhances the surgeon's FoV, it does not provide guidance on how to best aim the catheter.

To address this, we designed NeuroLens, *the first AR system that provided both the anatomical visualization of the patient's ventricular hologram and contextual guidance on catheter placement* to aid novice surgeons in learning about the EVD procedure and improving EVD placement accuracy. The AR guidance is enabled by the optical tracking of an external 6-camera OptiTrack system and visualized in AR by the Microsoft HoloLens 2, shown in Figure 1. We compute the transformation of world coordinates between OptiTrack and HoloLens 2, achieving high accuracy and low latency real-time tracking of optical markers in visualizing a patient-specific 3D model.

NeuroLens integrates contextual guidance, shown in Figure 1, that is enabled by tracking the EVD catheter [12]. The guidance consists of displaying the catheter's trajectory,

- *Sangjun Eom and Maria Gorlatova are with Department of Electrical and Computer Engineering, Duke University. E-mail: sangjun.eom, maria.gorlatova@duke.edu.*
- *Seijung Kim is with Department of Computer Science, Duke University. E-mail: seijung.kim@duke.edu.*
- *Joshua Jackson is with Department of Neurosurgery, Duke University. E-mail: joshua.jackson@duke.edu*
- *David Sykes is with School of Medicine, Duke University. E-mail: david.sykes@duke.edu.*
- *Shervin Rahimpour is with Department of Neurosurgery, University of Utah. E-mail: shervin.rahimpour@hsc.utah.edu*

angle of insertion, and distance to the target. In addition, we employ voice commands for surgeons to intra-operatively initiate and complete the procedure with ease, and personalize the anatomical visualization based on their needs. In our initial paper [12], we evaluated NeuroLens with 33 medical students under an Institutional Review Board (IRB)-approved study by comparing the AR-guided EVD trials to conventional freehand EVD trials. In this paper, we extended the evaluation by conducting an additional user study with 9 neurosurgeons using a new patient-specific phantom skull. We analyzed the tracking results of our OptiTrack setup between the two user studies and the EVD performance of students and surgeons with statistical analysis. Furthermore, we extended the analysis of qualitative data by adding survey responses from the surgeons and their additional feedback.

Our contributions are as follows:

- We design an optical marker-based AR system using 6 OptiTrack cameras and Microsoft HoloLens 2 for intra-operative use in neurosurgery. Our approach reduces image registration error to 1.17mm, outperforming state-of-the-art fiducial marker-based methods (Section 3).
- We integrate AR-based contextual guidance to aid surgeons in catheter targeting by displaying, in real time, the distance to the target, the angle of insertion, and the catheter projection. Additionally, we develop a patient-specific phantom model to evaluate NeuroLens in more realistic settings (Section 3). Our user study shows that the students agreed or strongly agreed with the usefulness of contextual guidance (97%) and the phantom model for learning (93.9%). Additionally, the surgeons agreed or strongly agreed that our setup will improve EVD training (88.9%) (Section 5).
- Our study demonstrated that NeuroLens improves students' and novice surgeons' accuracy more than an unassisted ('freehand') EVD procedure. The study also revealed important differences in the behavior of groups of students that achieved the best and the worst accuracy in NeuroLens-assisted EVD trials; specifically, we observed that the best-performing group took longer to complete the procedure, and focused on the contextual guidance substantially more than the worst-performing group (Section 5).

We first describe related work on image registration, tool tracking, and contextual guidance with AR in medical domains in Section 2. Then, we lay out the overall architecture in Section 3 and user study design in Section 4. We analyze the user study results in Section 5. Discussion and future work are presented in Section 6. Conclusions are given in Section 7.

2 Related Work

2.1 Marker-based Tracking

2.1.1 Image Registration

Fiducial and optical marker-based tracking is a common approach used to detect the position and orientation of an object in a surgical application. In AR-assisted surgery, marker-based tracking has been employed in the tracking of a surgical robot arm [45] and image registration of anatomical visualization in various types of surgery (e.g., open surgery [1], neurosurgery [14], [21], [48]). Prior work that used fiducial markers reported image registration errors ranging from 2.5mm to 8.5mm [13], [47] with drifts over time [14], [47]; with optical markers, smaller registration error of 1mm to 2mm was reported [11]. Hence, we designed NeuroLens to rely on optical markers for the image registration of a ventricular hologram on a patient's skull.

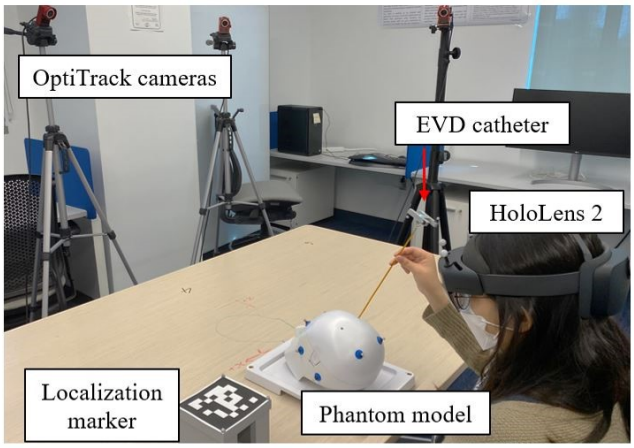

Fig. 1: The overall setup of NeuroLens

2.1.2 Tool Tracking

Due to the limited FoV and computational constraints of the head-mounted AR devices, marker-based tracking has been a standard approach for tool tracking over computer-vision-based techniques in AR-assisted neurosurgical applications. However, it is challenging to use fiducial markers for tracking a surgical tool due to the heightened sensitivity of fiducial marker detection algorithms to the angle and the distance between the AR device and the marker [5]. The uses of fiducial markers have been demonstrated in tracking rigid tools such as a robotic arm [45], laparoscope [64], or endoscope [28] secured in a fixed place with a static motion. Optical markers, on the other hand, can ensure more accurate tracking of the surgical tools that are mobile, not being fixed in one location. Prior studies of using optical markers in tracking rigid tools limit the area of tracking by the use of one camera, thus restricting the movement of tools in the large surgical areas [35], [48], [56], [67]. We configure the 360 degree FoV from 6 OptiTrack cameras in NeuroLens, surrounding the surgical area to maximize the area of tracking and ensure accurate tracking of various motions using the tools.

2.2 AR-assisted EVD

There has been an increasing interest in integrating AR into cranial-based procedures to provide additional anatomical and navigational information [6], [18], [24]. These AR-based assistance can be used for patient consultation [34], preoperative surgical planning [52], [56], and intra-operative surgical guidance [62]. One example of providing anatomical information in cranial-based procedures is to identify the anatomical landmarks of the patients [23] for a markerless

image registration [20], [30], [54]. This saves the preparation time and is easy to use on patients [34], however a larger registration error, ranging from 3mm to 5mm [3], [30], [42], was reported when compared to the marker-based image registration. The prime example of AR-based assistance in cranial-based procedures is the visualization of the target of the anatomy inside the skull to assist the targeting task through image registration [9]. This AR assistance can improve the distance to the target [22], [63], and reduces the attention shifts of surgeons' focus [29], when compared to a standard neuronavigation system with an additional navigation screen. EVD is an example of a challenging cranial-based procedure where surgeons have a limited FoV of targeting anatomy, thus relying on the patient's anatomical landmarks to estimate the location of the target point.

To improve the freehand EVD catheter placement accuracy, several researchers have developed systems that use AR to render a registered hologram of a patient's ventricles, enabling the surgeon to see the location they are targeting [11], [31], [47], [58]. A system for both cranial biopsy and EVD, reporting a sub-millimeter accuracy level, was proposed by [49]; however, the system did not use a head-mounted AR device, and a needle was used instead of the catheter for placement. Additionally, [58] demonstrated promising results in a study with 8 medical students which reported an average accuracy of 19.9mm for a freehand procedure and 11.9mm for an AR-assisted procedure, but much room for improvement remains, particularly for assisting surgeons with less experience in the procedure. NeuroLens improves upon the registration accuracy results reported in prior work, and integrates additional guidance to aid surgeons who are learning the procedure. Additionally, our evaluation of NeuroLens's AR assistance for EVD more than doubles the number of participants including both medical students and surgeons, compared to prior work (42 in our study vs. 8–15 in [31], [47], [58]), allowing us to draw unique insights about the differences in performance of different user groups.

To evaluate the performance of the EVD catheter placement in training, a realistic phantom model is required to provide accurate presentations of anatomical landmarks and brain-like texture [60], [65]. Prior studies show that a patient-specific phantom model can be generated by extracting a 3D skull model out of a patient's CT scans [36] and a realistic brain-like texture can be simulated through using Jell-O [4] or polyvinyl alcohol [27]. While polyvinyl alcohol creates a phantom with better ultrasound and x-ray contrasts [16], its texture is too firm, unlike the Jell-O, to be penetrated by the catheter to simulate the EVD. Thus, we 3D-print the skull by extracting the model from the same patient's CT scans as the ventricular model and placing a brain mold filled with a Jell-O mix to imitate the brain-like texture for more realistic EVD training. To our knowledge, we are the first to evaluate the brain texture made of Jell-O in AR-assisted EVD.

2.3 AR-based Contextual Guidance

Coupling AR-based visualizations of a patient's anatomy with additional contextual information about the surgical task has the potential to reduce the surgeon's cognitive

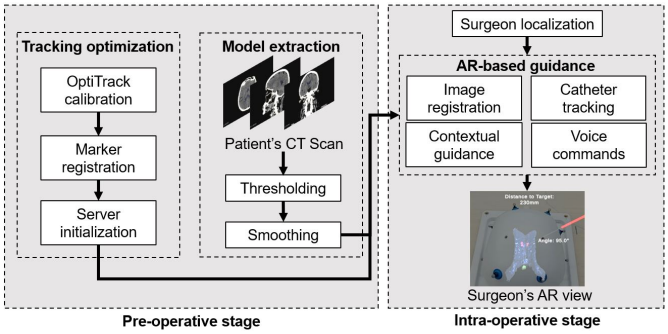

Fig. 2: Overall architecture of NeuroLens.

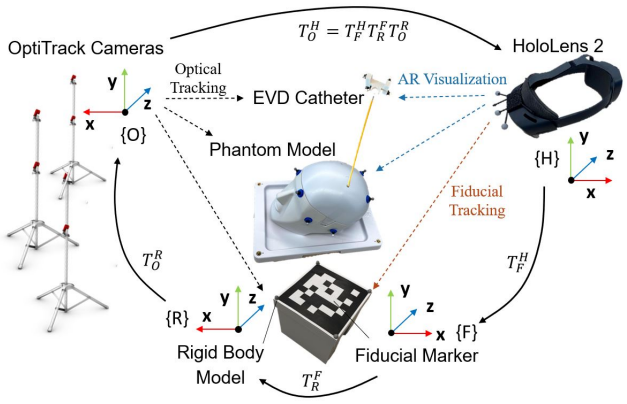

Fig. 3: System setup and transformation of world coordinate systems between OptiTrack and HoloLens 2.

workload and improve the outcomes of AR-supported surgeries [61]. Prior studies show that such contextual guidance can be implemented in surgical training by displaying instructional information for skill acquisition through tracking the user's eye gaze to detect the surgical performance [33], predicting currently performed surgical task to visualize information corresponding to the task through a neural network [10], or providing post-trial feedback to the users including scores on users' performance and areas that need more practice [66]. In intra-operative contextual guidance, different types of domain-specific contextual guidance have been demonstrated for AR-supported endodontic [51], dental implant [26], and orthopedic [57] surgeries. NeuroLens uniquely provides AR-based contextual guidance intra-operatively for EVD by visualizing contextual information about the catheter trajectory; we assess the impact of this guidance via quantitative and qualitative measures of surgeons' performance, experience, and engagement with different elements of the guidance.

3 Overall Architecture

Figure 2 shows our overall architecture in two stages. In the pre-operative stage, optimization of OptiTrack tracking and extraction of a patient-specific ventricular hologram are completed. In the intra-operative stage, the surgeon localizes for computing the transformation of world coordinates, and then initiates the AR-based guidance.

3.1 System Setup

NeuroLens uses the HoloLens 2 as the AR headset and six Flex 3 OptiTrack cameras with lens specs of 57.5 degrees in the FoV and 800nm of a long-pass infrared range for real-time tracking. The OptiTrack cameras are evenly distributed around the table to capture the full 360 degrees of an angular view for stable and accurate tracking of the optical markers. We use the OptiTrack cameras to track four objects including the HoloLens 2, the phantom model, the localization marker, and the EVD catheter, as shown in Figure 3.

3.1.1 Transformation of World Coordinates

HoloLens 2 and OptiTrack operate in different world coordinates, thus a transformation between those two coordinate systems is required. To compute the transformation of the world coordinates, both HoloLens 2 and OptiTrack locate the same target that serves as a reference point, a common approach to calculating the differences in coordinate systems when relying on an external optical tracking system [19], [46], [59]. We created a 12cm by 12cm square 2D fiducial marker as a localization target. This localization marker is detected by the HoloLens 2 Vuforia marker detection, which reported higher accuracy in registration error when compared to other detection methods (e.g., ARToolKit) [11], to obtain both the position and the orientation of the marker. Four optical markers were attached to the corners of the localization marker to be tracked by the OptiTrack system. The transformation of the world coordinates is shown in Eq. 1, where T_F^H is obtained by Vuforia marker detection on HoloLens 2, T_R^F is the transformation between the fiducial marker and a rigid-body of the optical marker, and T_O^R is obtained by OptiTrack's tracking of the localization marker:

$$T_O^H = T_F^H T_R^F T_O^R. \quad (1)$$

By computing the transformation of the world coordinates, NeuroLens ensures the robustness of the system through high accuracy of image registration and low latency of data communication between OptiTrack and HoloLens 2. The image registration error was calculated by running 15 trials of measuring differences in the displacement between the phantom model and the hologram in each axis with a digital caliper. The average image registration error of the three axes was 1.17mm. The average latency of data communication between OptiTrack and HoloLens 2 was 12.32ms. This improves upon prior work on image registration using a fiducial marker tracking [13], [47] that reports over 2mm of registration error.

3.2 Phantom Model

We created two phantom models: a standard skull model and a patient-specific 3D-printed skull, shown in Figure 4a and b, respectively. These phantom models are anatomically similar to a patient's head for testing, analysis, and evaluation of our system. We attached eight optical markers to both phantom models to facilitate real-time tracking by the OptiTrack system. We pre-drilled holes on both phantom models corresponding to Kocher's points which are the external landmarks that serve as entry points for the EVD catheter placement. A 3D printable brain mold was designed to be placed within the phantom models where a metal bead was located at a target of the foramen of Monro. This allowed the accuracy of catheter placement to be analyzed by measuring the distance between the tip of the catheter and the foramen of Monro on a post-experiment micro CT scan. The CT scans can be used to visualize both the catheter tip and radiopaque foramen of Monro (additional details are provided in Section 5).

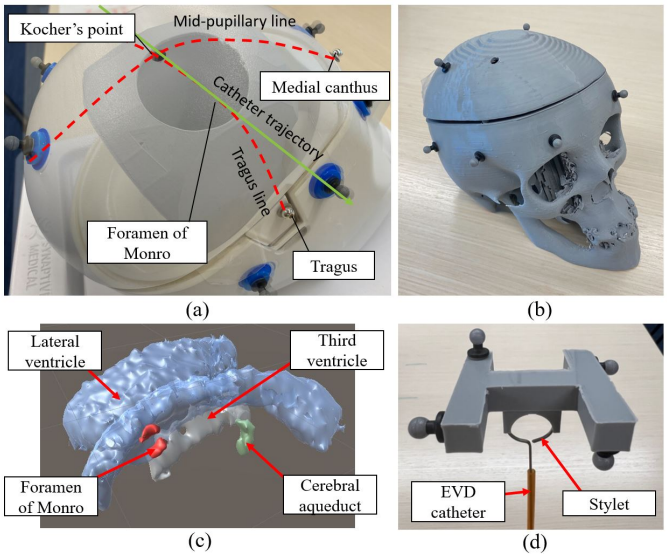

Fig. 4: Anatomical landmarks on a standard phantom model (a), 3D-printed patient-specific skull model (b), patient-specific ventricular hologram consisting of four different parts (c), and a custom 3D-printed mount for catheter tracking (d).

3.2.1 Patient-specific Skull Model

To create a patient-specific phantom model [36], we extracted a 3D model from the anonymous patient's computer tomography (CT) scan, using the 3D Slicer software. We applied a threshold to extract the bone structures, and a smoothing filter to the whole surface to render the 3D model to be 3D-printable with less number of contours. We cut the model into two parts: top and bottom to be able to open and close the skull. The inside of the skull model is hollow, allowing a 3D-printable brain mold to sit in. We attached a peg for the brain mold to secure its position. The 3D-printed patient-specific skull model is shown in Figure 4b with identifiable anatomical landmarks. Thus, the locations of the medial canthus and tragus were not necessary to be marked on the model. Both left and right Kocher's points were pre-drilled on the top part of the skull model.

3.2.2 Patient-specific Ventricular Hologram

To achieve a more realistic target of ventricular hologram in AR, we extracted a sample model of brain ventricles from the same patient's CT scan which we extracted a skull model from. Using 3D Slicer software, we applied a threshold to extract the ventricles, a smoothing filter to render the 3D ventricular model, and labeling of each ventricular part on the model. Our ventricular model, shown in Figure 4c, includes a lateral ventricle, two foramen of Monro, a third ventricle, and a cerebral aqueduct. The right foramen of

Monro was used as a target point of the catheter placement during the user study.

3.2.3 Brain Texture

To simulate a realistic, brain-like texture within the mold, we created two solutions to be evaluated in our user studies. The first solution was using an agarose gel, commonly used for electrophoresis in biochemistry, made from a solution of molecular biology grade agarose powder and water at a ratio that was optimized for creating a firm texture. This solution was firm enough to hold the catheter, yet still penetrable, hence it provided texture feedback during the catheter insertion. The solution for a single mold was made by combining 2.70g of agarose powder with 360ml of water. The solution was stirred, and then heated to boil, allowing the agarose to dissolve. This solution was cooled for approximately 30 minutes before being poured into the mold, where it was left to solidify for 120 minutes. The entire process took about 160 minutes per mold. We used this solution with a standard phantom model for conducting user study with medical students. Similarly, we created a solution using a Jell-O mix with a concentration rate of 12.5% [36] to create a more realistic texture than an agarose solution. This solution was made with the same procedure of creating an agarose solution and used for conducting user study with surgeons.

3.3 Voice Recognition and Personalization

We used the built-in voice recognition on HoloLens 2 to allow surgeons to initialize, complete the EVD procedure, and personalize the anatomical visualization of a ventricular hologram. The surgeons used the voice command, "*start*," to compute the transformation of world coordinates when a fiducial marker was detected. When the catheter placement was completed, the surgeons used the voice command, "*complete*," to record the resulting catheter placement before removing the inner stylet. The voice command was used as a complimentary feature for participants to record the starting and completion points of the procedure for data analysis.

We also provided a list of voice commands to allow surgeons to personalize the anatomical visualization of a ventricular hologram based on their needs. Often, when complicated medical information is visualized in AR, the surgeon's view could be obstructed, hence the obstruction of view could make it harder to visualize the target. This could potentially increase discomfort such as fatigue from the visualization. By default, all four parts of the hologram, shown in Figure 5a, are visualized; however, we allowed surgeons to hide its parts by using the voice command, "*hide*," followed by the name of the parts such as the "*third ventricle*" or the "*lateral ventricle*".

3.4 Tool Tracking and Contextual Guidance

We integrated AR-based contextual guidance by tracking the EVD catheter to aid the catheter projection and the targeting of the foramen of Monro. We determined these types of guidance based on prior experiences and expertise from our team consisting of two expert neurosurgeons (one fellow and one senior resident with experience in teaching and performing the EVD procedure) and one senior neurosurgery medical student (with prior experience in EVD training).

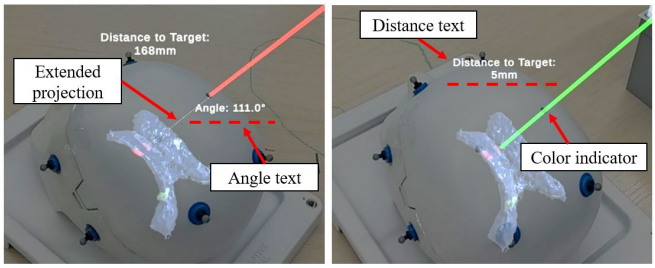

(a) (b)

Fig. 5: AR-based contextual guidance estimating catheter trajectory (a) and targeting foramen of Monro (b).

3.4.1 Catheter Tracking

The EVD catheter is a thin flexible tube about 36cm in length and 3mm in diameter. An inner stylet is inserted inside the catheter to provide stiffness to the catheter placement task. Attaching optical markers to a catheter itself is impractical because of its dimensions and elasticity. Thus, we designed an H-shape 3D-printed mount with the dimensions of 50mm by 50mm by 10mm to be latched at the top of the inner stylet, shown in Figure 4d. This mount added a 9.5g of weight to the EVD catheter and inner stylet which did not cause any detrimental workloads such as bending. We attached four optical markers to each corner of the H-shape to provide enough distance between markers to avoid occlusions or false positive tracking of the markers.

3.4.2 Aiding Catheter Projection

During the insertion of the catheter through a skull, the direction of the catheter is critical to determining whether the catheter will hit the foramen of Monro. However, due to the limited FoV inside the skull, surgeons face difficulties in estimating a catheter trajectory that lines up with the target. We create an AR visualization of an extended line of a catheter projection as a white dotted line in a 3D hologram to aid the surgeons. This helps surgeons in estimating the catheter projection inside the skull and aligning the catheter to be in line with the target, as shown in Figure 5b.

Another contextual element is a textual indicator of the angle, θ, between the catheter hologram and the surface of the skull. This angle of catheter insertion determines whether the trajectory of the catheter is in line with the foramen of Monro. The approximate angle of catheter trajectory for a freehand EVD is about 90 degrees to the surface of the skull [17]. We use Eq. 2 to calculate this insertion angle relative to the skull by using vectors of catheter hologram, v_c, and the surface of the skull, v_s.

$$\theta = cos^{-1}\left(\frac{v_c \cdot v_s}{|v_c|\,|v_s|}\right). \tag{2}$$

We visualize the angle as a textual indicator in AR below Kocher's point, as shown in Figure 5a.

3.4.3 Targeting the Foramen of Monro

While visualizing the catheter projection guides the surgeons in determining the right insertion angle of the

catheter, we also display the depth of catheter insertion by calculating the Euclidean distance $d(C,T)$ between the tip of the catheter, (x_c, y_c, z_c), and the foramen of Monro, (x_t, y_t, z_t), using Eq. 3, and displaying this distance as a textual indicator above the ventricular hologram, as shown in Figure 5b.

$$d(C,T) = \sqrt{(x_c - x_t)^2 + (y_c - y_t)^2 + (z_c - z_t)^2}. \quad (3)$$

With this textual indicator, surgeons no longer need to read the depth label physically marked on the catheter, and can instead maintain their focus on the surgical area.

Another contextual element comes from a color indicator of the catheter hologram that shows whether the foramen of Monro is in line with the catheter projection. To calculate the distance from the foramen of Monro to the catheter projection, $d(C_t, C_b, T)$, a point-to-line Eq. 4 is used, where C_t is the 3D coordinate of the top of the catheter, C_b is the 3D coordinate of the tip of the catheter, and T is the 3D coordinate of the foramen of Monro.

$$d(C_t, C_b, T) = \frac{|(C_t - T) \times (C_t - C_b)|}{|C_b - T|}. \quad (4)$$

The threshold of the distance is set to 2mm. This means when $d(C_t, C_b, T) < 2$mm, the catheter hologram changes color to green to indicate that the catheter is projected to end up in close proximity to the foramen of Monro. When $d(C_t, C_b, T) > 2$mm, the color of the catheter hologram stays red.

4 User Study Design

Our study, approved by the Duke University IRB, was centered on medical students and surgeons performing freehand EVD trials, followed by AR-assisted EVD trials. We asked each medical student to perform one freehand EVD trial, followed by one AR-assisted EVD trial. Prior to each trial, each medical student was provided with an instructional video. For surgeons, we asked each of them to perform two freehand EVD trials, followed by two AR-assisted EVD trials. The shortened description of verbal instructions was given to surgeons, instead of the videos.

4.1 EVD Trials

4.1.1 Freehand EVD

The steps for freehand placement of an EVD are as follows. Kocher's point was approximated by locating two key anatomical landmarks: the tragus and the medial canthus as shown in Figure 4a. The point on the skull in which a sagittal plane through the medial canthus intersects a coronal plane through the tragus was defined as Kocher's point. Next, the target point of the foramen of Monro was approximated by angling the catheter tip from Kocher's point towards the contralateral medial canthus. The catheter was inserted approximately 7cm towards the target, and finally, the inner stylet was removed. These steps were described in an instructional video[1] recorded by a neurosurgeon with 8 years of clinical experience. The instructional video was 90 seconds long. A full length of the instructional video was used for the user study with medical students while a shortened verbal instruction was used for surgeons to target the right foramen of Monro through the right Kocher's point due to their prior knowledge of freehand EVD procedure. Each medical student performed one freehand EVD trial on the standard phantom model shown in Figure 4a, and each surgeon performed two freehand EVD trials on the patient-specific phantom model shown in Figure 4b.

4.1.2 AR-assisted EVD

The steps of an AR-assisted EVD were as follows. First, eye calibration on HoloLens 2 was performed to render holograms at accurate locations to ensure the consistency of image registration and collect accurate eye gaze data. Upon the initialization of the AR app on HoloLens 2, the localization marker was detected and a cube hologram was overlaid on top of the localization marker. We verbally asked the participants whether the cube hologram was overlaid on an accurate location to keep the computation of the transformation of world coordinates consistent throughout the study. The AR visualization and guidance were initiated through a voice command issued by the user. Next, the catheter was inserted into a target point, and finally, the inner stylet was removed. These steps were described to participants in an instructional video[2] created by a team with a combination of AR and neurosurgical expertise. The instructional video was 180 seconds long. This instructional video was used for the user study with medical students while shortened verbal instructions were used for the user study with surgeons due to their prior knowledge of EVD. Each medical student performed one AR-assisted EVD trial on the standard phantom model shown in Figure 4a, and each surgeon performed two AR-assisted EVD trials on the patient-specific phantom model shown in Figure 4b.

4.2 Survey Questions

The pre-experiment and post-experiment surveys were given to each participant to fill out before and after the user study. In the pre-experiment survey, we asked demographic questions about prior experience in AR and EVD. We assembled a set of questions in six different categories for the post-experiment survey formulated in coordination with expert neurosurgeons and reference from prior research in AR-assisted EVD [58], shown in Table 1. The first five categories, AR visualization, contextual guidance, AR experience, surgical experience, and physical discomfort were given to both medical students and surgeons. The last category, educational value, was only given to surgeons.

For the category of AR visualization (Q1−Q4), we asked the participants if each hologram was realistic and if overall visualization was useful for learning. For the category of contextual guidance (Q5−Q11), we asked the participants if each type of contextual guidance was useful and if overall contextual guidance was useful for learning. For the categories of AR (Q12−Q14) and surgical experiences (Q15−Q18), we asked the participants if the system was robust without lagging, drift, and obstruction of view, and

1. The instructional video of a freehand EVD is provided at https://youtu.be/wCKOd4m7jK4

2. The instructional video of an AR-assisted EVD is provided at https://youtu.be/O3OEadllqWM

TABLE 1: Post-experiment survey questions.

	Questions
Q1	The ventricular hologram in AR environment was realistic.
Q2	The catheter hologram in AR environment was realistic.
Q3	The positioning of the foramen of Monro in AR environment was realistic.
Q4	The overall AR-based visualization was useful for learning about the neurosurgical procedure.
Q5	The extended projection of catheter (a white dotted line) in AR environment was useful.
Q6	The color indicator of catheter projection (red/green catheter holograms) in AR environment was useful.
Q7	The text showing distance from the tip of catheter to foramen of Monro in AR environment was useful.
Q8	The text showing the angle between the catheter projection and surface of the phantom model in AR environment was useful.
Q9	The voice commands in AR environment were useful.
Q10	The personalization of hologram (e.g. hiding and showing parts of ventricular hologram via voice commands based on personal needs) was useful.
Q11	The overall AR-based contextual guidance was useful for learning about the neurosurgical procedure.
Q12	The hologram visualization was robust without significant lagging.
Q13	The hologram visualization was robust without significant drift or jump.
Q14	The hologram visualization didn't obstruct my view.
Q15	The phantom model was realistic.
Q16	The texture feedback (during catheter insertion procedure) inside the phantom model was realistic.
Q17	The use of phantom models was useful for learning about the neurosurgical procedure.
Q18	AR guidance will be helpful in clinical settings intra-operatively.
Q19	I didn't feel tired or fatigued at some point during the experiment.
Q20	I didn't feel dizziness at some point during the experiment.
Q21	I didn't feel discomfort with the AR headset at some point during the experiment.
Q22	The AR system is appropriate to teach the EVD procedure.
Q23	The AR system is easy to use for the EVD training.
Q24	The AR system improves the EVD training.
Q25	What was the most challenging task of the external ventricular drain procedure?
Q26	If you have any other comments or feedback about your experience, please write below.

if the phantom model was useful for learning. For the category of physical discomfort (Q19−Q21), we asked the participants if they experienced fatigue, dizziness, and discomfort. Lastly, for the category of EVD training (Q22−Q24), we asked the participants if the AR system is appropriate to teach, easy to use, or brings improvements to the EVD training. All questions in these six categories are answered on a five-point Likert scale. At the end of the survey, we asked the participants to identify the most challenging task of the EVD and to leave any open-ended feedback about the overall experience (Q25 and Q26).

4.3 Data Collection

During both freehand and AR-assisted EVD trials, we collected data on the total completion time of the procedure and the accuracy of the catheter distance to the target. Additionally, during the AR-assisted trials, we captured the participants' eye gaze distribution.

4.3.1 Total Completion Time

We measured the total completion time of the freehand EVD trial with a stopwatch from the moment that the participant started identifying the anatomical landmarks to the removal of the inner stylet. The total completion time of the AR-assisted EVD trial was measured by the system from the moment that the AR app was initialized to the removal of the inner stylet.

4.3.2 Distance to the Target

Since the optimal catheter trajectory is a straight line from the entry point (i.e., Kocher's point) to the foramen of Monro to avoid hitting other key areas of the brain, we recorded a distance to target (i.e., the 3D Euclidean distance from the tip of the catheter to the foramen of Monro) for the evaluation of the EVD placement accuracy. The distance to target is a standard method of evaluating catheter placement as commonly examined in prior AR-assisted EVD [31], [47], [58]. To obtain an accurate distance to target inside the mold, we used a Nikon XTH 225 ST, a high-resolution micro X-ray CT scanner [50], to capture the full volume of the mold. After we obtained a sequence of more than one thousand slices of CT images, we visualized them in the 3D graphical software, Avizo, to render the 3D volume. The accuracy was calculated by measuring the Euclidean distance from the target point of the metal bead to the tip of the catheter.

4.3.3 Eye Gaze Distribution

We enabled the built-in gaze tracking on HoloLens 2 to collect the gaze direction during each AR-assisted EVD trial. Using the gaze direction, we calculated the gaze hit point on the hologram to measure the distribution of the participant's gaze focus. We segmented the holograms into four categories of the ventricle, the EVD catheter, the distance text, and the angle text, and analyzed the distribution of the participant's gaze focus on each category. All eye gaze data were collected from the AR-assisted trials using the standard phantom model to keep the consistency of the experimental setup for AR-assisted EVD simulation.

4.4 Participant Selection

We recruited 33 medical students from Duke University, Durham, NC, USA, and the University of North Carolina, Chapel Hill, NC, USA, and 9 neurosurgeons from the Department of Neurosurgery at Duke University Hospital, Durham, NC, USA.

4.4.1 Selection of Medical Students

We had 19 year 1 students and 14 year 2−4 students with clinical experience. All 33 students had no knowledge of the EVD procedure. One of them uses the AR headset infrequently, less than once a week, 15 had worn an AR headset once or twice, and 17 had never worn an AR headset. 20 of them wore glasses for nearsightedness and 13 did not; none of the participants had any other eyesight-related conditions such as strabismus or colorblindness.

4.4.2 Selection of Neurosurgeons

We had 8 residents with neurosurgical experiences ranging from 1 to 7 years, and 1 fellow with 20 years of neurosurgical experience. The number of EVDs that neurosurgeons have performed in the past varied from 5 to 250 and was correlated to their number of years of neurosurgical experience. 6 of them have used the AR device once or twice, and 3 of them have never used the AR device.

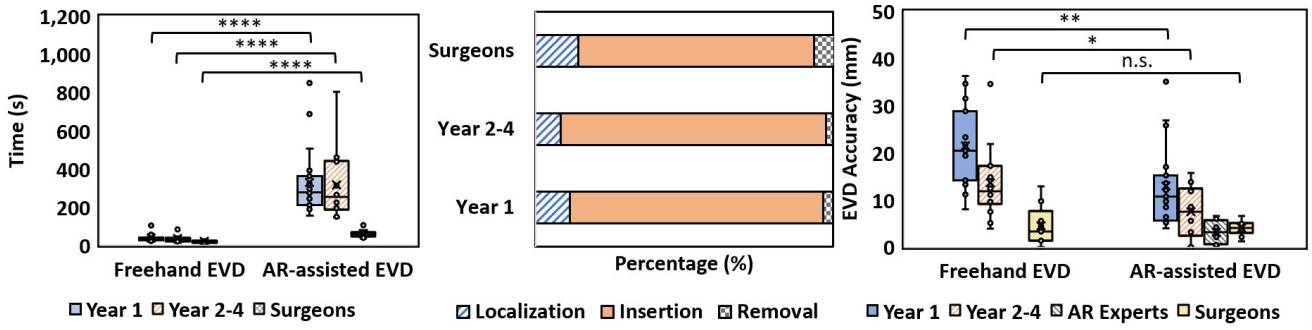

Fig. 6: Average EVD completion time (a), average percentage of total time spent on each task (b), and average accuracy in catheter distance to the target (c). n.s.: no statistical significance, (*): $p \leq 0.05$, (**): $p \leq 0.01$, (***): $p \leq 0.001$, and (****): $p \leq 0.0001$.

(a) (b)

Fig. 7: System setup in our research lab for the user study with medical students (a) and setup in Duke Hospital room for the user study with surgeons (b).

TABLE 2: OptiTrack calibration results for user studies.

	User Studies	
Number of Days of Experiment	13	3
Target Participant	Students	Surgeons
Number of Participants	33	9
Mean 3D Error (mm)	0.348 ± 0.047	0.740 ± 0.036
Mean 2D Error (pixels)	0.112 ± 0.016	0.134 ± 0.006

5 Results

5.1 OptiTrack Calibration

The calibration results of OptiTrack real-time tracking for both user studies are shown in Table 2. We conducted both user studies across multiple days (i.e., a total of 16 days) in which we calibrated the OptiTrack system each day to ensure the optimization of tracking. The user study with medical students was conducted in our research lab (shown in Figure 7a) at the Duke University campus, while the user study with surgeons was conducted in the Duke Hospital break room (shown in Figure 7b). The overall mean 3D error (0.348mm) and 2D error (0.112 pixels) in the user study with medical students were lower than the mean 3D error (0.740mm) and 2D error (0.134 pixels) in the user study with surgeons. This was due to the space constraint of the Duke Hospital break room which provided a smaller space than our research lab to set up our system. The OptiTrack cameras were distributed at a shorter distance around the surgical area, covering less space for tracking, thus resulting in higher mean 3D and 2D errors of calibration. The OptiTrack calibration results reflected the accuracy of optical marker tracking and validated whether the setup was appropriate for optimal tracking or not. While we hypothesize that these calibration results may have had impacts on the robustness of image registration and tool tracking, both setups achieved sub-mm tracking accuracy, which was equivalent to the best calibration rating (i.e., exceptional) on OptiTrack software, ensuring robust image registration across the two studies.

5.2 EVD Completion Time

Year 1 students spent more time on the freehand EVD trial (37.36s) than the year 2−4 students (34.73s). Similarly, the completion time of the AR-assisted EVD trial for the year 1 students (329.56s) was longer than for the year 2−4 students (313.45s), as shown in Figure 6a. The differences in completion time between the freehand EVD and AR-assisted EVD trials were statistically significant for both year 1 students ($p \leq 0.0001$) and year 2−4 students ($p \leq 0.0001$). There was a larger difference in the total completion times between these two groups in the AR-assisted EVD trial than in the freehand trial. We hypothesize that, since the year 2−4 students had clinical experience, they were better at ensuring the accuracy of the catheter alignment and understanding each element of contextual guidance, which resulted in shorter completion times. Furthermore, both groups spent more time in the AR-assisted EVD trial than in the freehand EVD trial. We hypothesize that since almost all medical students have neither performed the EVD procedure nor used AR technology in the past, they spent more time learning about how to use AR guidance and apply it to learning about the EVD procedure.

Similarly, the completion of the AR-assisted EVD trial was longer than the freehand EVD trial for the surgeons. On average, the surgeons spent more time on the AR-assisted trial (59.1s) than the freehand EVD trial (18.0s). This difference was statistically significant with a two-tailed Student's t-test ($p \leq 0.0001$). This was reasonable to expect since the surgeons had more clinical experience and knowledge of the EVD procedure than the students. As the AR-assisted EVD trial consists of three tasks, localization, catheter insertion, and inner stylet removal, we analyze the time distribution on these tasks; these results are shown in Figure 6b. Overall, the year 1, the year 2−4 students and surgeons all spent a similar percentage of their time on localization, insertion, and removal.

TABLE 3: Comparison of NeuroLens to other AR-assisted EVD systems.

	Gestel et al. [58]	**Schneider et al. [47]**	**Li et al. [31]**	**NeuroLens** (this paper)			
Image Registration	Yes	Yes	Yes	Yes			
Tool Tracking	Rigid	No	No	Non-rigid			
Contextual Guidance	No	No	No	Yes			
Hardware	HoloLens 1	HoloLens 1	HoloLens 1	HoloLens 2			
Registration Marker	Optical	Fiducial	Manual	Optical			
Surgical Tool	Needle	EVD catheter	EVD catheter	EVD catheter			
Phantom Model	Custom skull	Custom skull	Patient	Standard	Standard	Patient-specific skull	Standard
Brain Texture	Polyurethane	Agar	Patient	Agarose	Agarose	Jell-O	Agarose
Level of Expertise	Year 2−3 students	Surgeons	Surgeons	Year 1 students	Year 2−4 students	Surgeons	AR experts
Number of Participants	8	10	15	19	14	9	2
Freehand Accuracy (mm)	19.9 ± 4.2	N/A	11.26 ± 4.83	21.42 ± 8.08	13.55 ± 7.81	4.37 ± 4.65	N/A
AR-assisted Accuracy (mm)	11.9 ± 4.7	7.1 ± 4.1	4.34 ± 1.63	12.97 ± 8.54	7.36 ± 5.55	3.64 ± 2.48	3.12 ± 2.53
Accuracy Improvement (%)	40.2	N/A	61.5	39.4	45.7	16.7	N/A

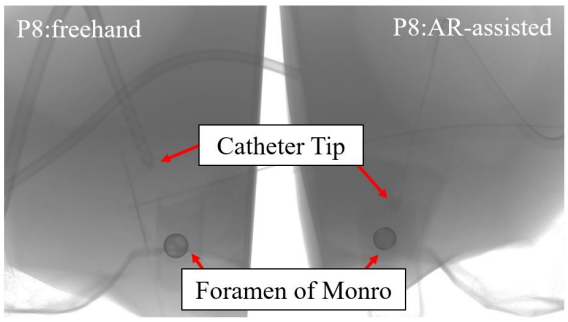

Fig. 8: A sample image of micro CT scans in coronal plane from the same participant's EVD trials: freehand (left) and AR-assisted (right).

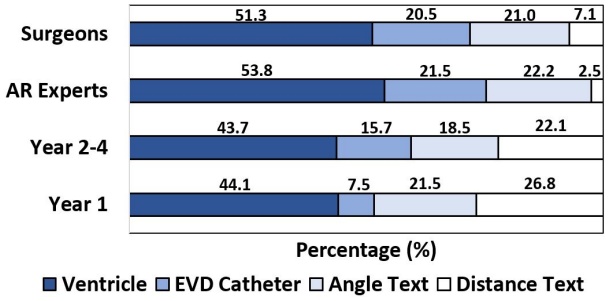

Fig. 9: Eye gaze distributions across holograms.

5.3 EVD Catheter Placement Accuracy

From the analysis, we found that the average Euclidean distance to the target on freehand EVD trials was 21.42mm for the year 1 students and 13.55mm for the year 2−4 students, as shown in Figure 6c. *On AR-assisted trials, this distance was reduced, on average, by 39.4% for the year 1 students and by 45.7% for the year 2−4 students*. These improvements were statistically significant with a two-tailed Student's t-test for both year 1 (p = 0.0090) and year 2−4 students (p = 0.0296). On the other hand, we found that the surgeons improved the distance by 16.7% on average, reducing from 4.37mm on the freehand trials to 3.64mm on the AR-assisted trials; however, this improvement was not statistically significant. A 2-dimensional sample slice of raw CT scan images is shown in Figure 8. The demonstrated accuracy improvements indicate the potential of NeuroLens to aid students and surgeons in reaching targets within the brain.

5.3.1 Comparison to the State of the Art

Table 3 shows the comparison of our results to the state of the art [31], [47], [58]. *The accuracy levels achieved by the NeuroLens-assisted AR experts considerably improved upon the best results presented in prior work* (i.e., reduce the average distance to the target by 28.1%, from 4.34mm reported in [31] to 3.12mm). This suggests that additional practice with NeuroLens would allow surgeons and medical students to improve upon the accuracy reported in this study; we will evaluate this in our future work. *Moreover, the accuracy levels achieved by the NeuroLens-assisted surgeons (3.64mm) were the best among the results from prior studies* (vs. 7.1mm [47], 4.34mm [31]).

Prior studies have not involved year 1 students; in our study, the extent of their accuracy improvement, between the freehand and the AR-assisted EVD trials, is at the level of the improvements observed in year 2-3 students in [58] (39.4% vs. 40.2%, correspondingly). On the absolute accuracy measurements, the year 1 students in our study performed worse than upper-year students in both prior studies and our work. However, the year 2-4 students' accuracy in our trials (7.36mm) significantly surpasses the accuracy achieved by upper-year students (vs. 11.9mm in [58]) and is comparable to the accuracy achieved by experienced surgeons (vs. 7.1mm in [47]) in previous work. Compared to prior work using HoloLens 1, the use of newer hardware (i.e., HoloLens 2) enhanced the quality of marker-based image registration.

5.4 Eye Gaze Distributions

From the eye gaze data collected in our user study, we calculated participants' distribution of eye gaze across the holograms during AR-assisted EVD trials; these results are shown in Figure 9. The four holograms used in this analysis were the ventricle, the EVD catheter, and the contextual guidance that comprises the angle text and the distance text. We did not make distinctions of eye gaze focus between the skull phantom and the ventricular hologram because the participants did not need to identify the landmarks on the skull during the AR-assisted trials. The ventricular hologram provided the location of the target point, hence participants were able to perform the EVD without focusing on other parts of the skull.

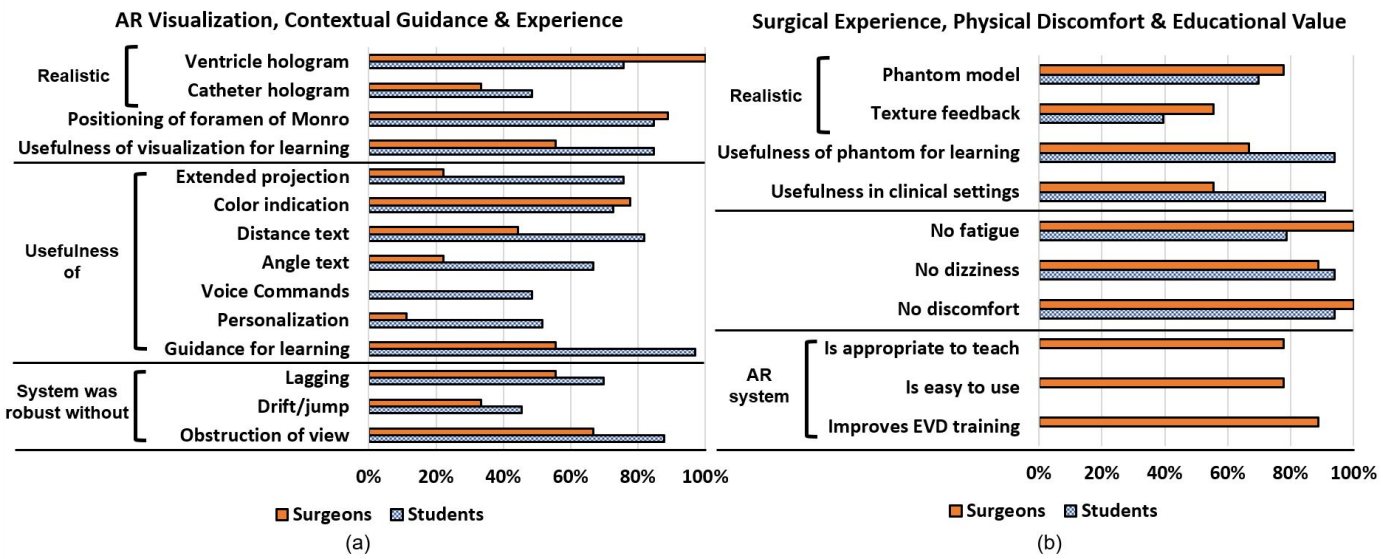

Fig. 10: Survey responses on positivity rates of AR visualization, contextual guidance, and AR experience (a), and surgical experience, physical discomfort, and educational value (b).

Across all levels of expertise, the participants dedicated considerable attention to the ventricular hologram, with the average percentage of time devoted to it varying from 43.7% for the year 2−4 students to 53.8% for the AR experts. *This indicates the importance of providing anatomical visualizations in AR-assisted surgery*. The extent of participants' attention dedicated to the contextual guidance presented by NeuroLens varied substantially by the participant's level of expertise: specifically, students looked at it considerably more than experienced surgeons or AR experts. Specifically, while the surgeons and the AR experts focused on contextual guidance for a total of, correspondingly, 28.1% of the time (21.0% on angle text, 7.1% on distance text) and 24.7% of the time (22.2% on angle text, 2.5% on distance text), the year 1 students focused on it for 48.3% of the time (21.5% on angle text, 26.8% on distance text), and the year 2−4 students for 40.6% of the time (22.1% on angle text, 18.5% on distance text). This is unsurprising: it is reasonable to expect less experienced participants to rely more on the guidance provided to them. In Section 5.6, we further analyze the differences in eye gaze patterns of students who achieve different levels of accuracy in their trials.

5.5 Survey Responses

Our post-experiment survey responses are summarized in Figure 10 with *positivity rates*. We define the positivity rate as the percentage of participants' responses in the "strongly agree" and "agree" categories. The participants' free-text responses are quoted with the participant number, *P* for students, and *S* for surgeons.

5.5.1 AR Visualization & Contextual Guidance

Both the students and the surgeons mostly agreed that the AR visualization of the ventricular hologram and positioning of the foramen of Monro was realistic (75.8% and 84.8% positivity rates for the students, and 100% and 88.9% positivity rates for the surgeons, correspondingly). *84.8% of the students agreed or strongly agreed that the overall AR visualization was useful for learning*, however a lower positivity rate (55.6%) was reported from the surgeons (and 44.4% of them responded with neutral). This shows the potential of using AR technology with realistic visualization of brain ventricles in EVD training for medical students. Only 48.5% of the students and 33.3% of the surgeons agreed that the catheter hologram was realistic. The students also provided additional feedback that they felt aligning the catheter hologram to the real catheter (P8, P9, P10, P13, P25, P27, P28, P33) or correcting the insertion angle (P11, P21) was difficult. Furthermore, a couple of surgeons provided additional feedback that the catheter projection did not match the freehand EVD projection (S1, S5, S8). This was due to the non-rigidity of the catheter which tended to bend depending on the way the catheter was held by the participants. While a standard technique is recommended to minimize the bending, there are still variations of tool handling (e.g., location of grabbing points or use of two hands versus one hand) among surgeons. In future work, we will explore the use of sensors (e.g., strain gauge or inertial measurement unit) on the catheter to detect the non-rigidity and reflect the accurate shape of the catheter hologram.

The students appreciated all forms of the contextual guidance we provided. The students agreed that the contextual guidance was useful, with high positivity rates for each of the elements: distance text (81.8%), color indication (72.7%), extended projection (75.8%), and angle text (66.7%). *97% of students agreed or strongly agreed that the provided contextual guidance was useful for learning*. This shows how helpful AR-based contextual guidance can be for medical students in learning about the EVD procedure and improving accuracy. However, a smaller number of the surgeons agreed or strongly agreed that each element of the contextual guidance was useful, with lower positivity rates: distance text (44.4%), extended projection (22.2%), and angle text (22.2%), except the color indication (77.8%). We hypothesize that this was due to the surgeons' level of

expertise in knowing all steps of the EVD procedure. Although the color indicator helped them recognize whether the catheter projection hit the foramen of Monro or not, the other textual indicators were not necessary for them to perform the EVD procedure. The students who provided additional feedback felt that "aligning the catheter hologram with green color" (P22, P23, P24) was the most challenging contextual guidance. This was potentially due to the low threshold of color indicator or unsteady hand movement making it difficult to keep it under the threshold. In future work, we will explore altering this guidance: e.g., converting a color-based indicator to a textual indicator, or allowing surgeons to turn it on and off.

The least appreciated elements of NeuroLens were the hologram personalization and the voice commands (51.5% and 48.5% positivity rates, correspondingly for the students, and 11.1% and 0% positive rates, correspondingly for the surgeons). Though the voice commands were available to surgeons for personalizing the anatomical visualization, the majority of the surgeons were satisfied with the ventricular hologram and did not choose to personalize it. This was due to the simplicity of the EVD procedure. We expect hologram personalization to be more important for other, more complex, AR-supported surgical settings: in our trials, the participants did not personalize holograms as the ventricular hologram provided sufficient information and none of the ventricular parts obstructed the surgical area. While we believe that voice commands will have an important role in AR-assisted surgery of the future, their usability in NeuroLens was limited by their lack of robustness: in our trials, the performance of the built-in voice recognition in HoloLens 2 was highly dependable on the noise in the environment, which required many participants to repeat voice commands, often multiple times.

5.5.2 AR & Surgical Experience

The students largely agreed that the provided visualizations did not obstruct their FoV (positivity rate: 87.9%), and that there was no noticeable lag in the system (positivity rate: 69.7%). However, a smaller number of the surgeons agreed or strongly agreed that the provided visualizations did not obstruct their FoV (positivity rate: 66.7%) and that there was no noticeable lag in the system (positivity rate: 55.6%). One surgeon also mentioned in the additional feedback that the text and image holograms were obscuring the view too much (S2). Due to focusing on the small region of the skull near Kocher's point, the AR visualization could lead to obstruction of view or visual clutter. We hypothesize that the participants' perception of AR visualization depended on their level of expertise. Expert surgeons might not need all contextual information about catheter tracking while students appreciated that contextual guidance helped improve accuracy. A significant number of the students (positivity rate: 45.5%) and the surgeons (positivity rate: 33.3%) observed drifting or jumping of the rendered virtual contents. In the open-ended feedback, some students additionally noted that they felt the catheter hologram "jumped" (P3, P14) and that it was hard to keep it steady (P1, P6). From our observations, instances of drifting or jumping were associated with specific scenarios, such as tracked objects coming in close proximity to one another or optical markers being blocked by the user; the prevalence of these scenarios was highly dependent on a specific participant's approach to catheter placement. In future work, we will further investigate these scenarios, and will examine to what extent they can be addressed via technical solutions (e.g., further optimizing placement of the markers and the OptiTrack cameras) and via providing additional instructions to the users of our system (e.g., instructing the users to avoid obstructing the markers).

5.5.3 Physical Discomfort

The standard EVD procedure of inserting a catheter is relatively brief (around 1 minute), hence we did not expect much discomfort or fatigue from using our AR system. By and large, the students agreed or strongly agreed that the system was robust without discomfort (positivity rate: 93.9%), dizziness (positivity rate: 93.9%), and fatigue (positivity rate: 78.8%). Similarly, the surgeons largely agreed that the system was robust without discomfort (positivity rate: 100%), dizziness (positivity rate: 88.9%), and fatigue (positivity rate: 100%). However, the positivity rate of the students for not experiencing fatigue in NeuroLens was lower and comparable to another reported AR-assisted EVD system (75% - "visual fatigue") [58]. We hypothesize that the high positivity rates of both students and surgeons not experiencing fatigue were due to the small region of focus around the skull minimizing the participants' movements and the short completion time of the procedure. We also hypothesize that there is a possibility of more fatigue if they spent more time completing the AR-assisted EVD trials [47] or if the surgical procedure was more complex with more steps and a larger region of focus. In future work, we will explore specific types of fatigue experienced by NeuroLens users (e.g., it could be associated with eye discomfort, or with wearing an uncomfortably-fitting headset), and will develop approaches for addressing it. For example, we could provide users with instructions to rest or reduce the amount of visual information presented to the users based on their level of fatigue.

5.5.4 Educational Value

The students mostly agreed with the usefulness of NeuroLens in clinical settings (positivity rate: 90.0%) and the usefulness of the phantom model for learning (positivity rate: 93.9%), while surgeons responded with lower positivity rates of 55.6% and 66.7%, respectively. We believe this is because the surgeons have more neurosurgical experience, which allowed them to identify the limitations of our system. However, a higher number of students agreeing with the usefulness of our system shows the potential of NeuroLens and its AR-based simulation using the phantom model as a future training tool for EVD training. Additionally, 69.7% of the students agreed or strongly agreed that our phantom model was realistic, while 77.8% of the surgeons agreed or strongly agreed. This was due to the change in the phantom models used in the user studies. The patient-specific phantom model (shown in Figure 4b) was expected to be more realistic than the standard phantom model (shown in Figure 4a). The change in the brain texture also resulted in a higher number of surgeons (positivity rate: 55.6%) agreeing that the phantom model was realistic

than students (positivity rate: 39.4%). In the open-ended feedback, one surgeon noted that "the texture feedback felt close to real" (S3). From the feedback, we believe that the 12.5% concentration Jell-O solution creates a more realistic imitation of brain texture than the agarose gel.

The surgeons largely agreed or strongly agreed that NeuroLens can be used for EVD training. The surgeons agreed that NeuroLens is appropriate to teach (positivity rate: 77.8%) and easy to use (positivity rate: 77.8%). *88.9% of the surgeons agreed that NeuroLens can improve EVD training*. This contrasts with the relatively lower positivity rate (55.6%) of the usefulness of NeuroLens in clinical settings. The difference in positivity rates was expected as there exist limitations for clinical implementation in NeuroLens (discussed in Section 6). Overall, *the surgeons agreed that the current form of NeuroLens is useful and suitable for EVD training*.

5.5.5 Additional Feedback

While participants' accuracy was, on average, considerably improved when NeuroLens was used (see Figure 6c), multiple students have indicated that the core challenges of accurate EVD placement do not fundamentally change with the addition of AR guidance: specifically, the participants felt that finding the correct depth (P2, P19, P26), getting to the correct angle of insertion (P4, P5, P15, P20, P29), and estimating the target location (P12, P18) were still challenging. This is intuitive: while the contextual guidance NeuroLens provides can help guide the surgeons' approach to the target and improve surgeons' accuracy, the core task of hitting a small target in an enclosed space through a narrow opening remains challenging.

Overwhelmingly, the participants were positive about AR as a technology and its potential impact on neurosurgical applications. The students thought the system was "a great, realistic tool for minimally invasive surgery" (P9), "great technology" (P15, P29), and "amazing tool for training, prep, and intra-operative use" (P17). One participant was "looking forward to seeing the technology progress" (P14). The students also stated that the experience was "really cool" (P1, P5, P20, P27), "very useful" (P5, P22, P33), a "great experiment" (P23), and a "great learning experience" (P1). The surgeons stated that "this tool has phenomenal potential" (S1), and "the technology has great potential" (S3). The enthusiasm of both medical students and surgeons further indicates NeuroLens's potential as an educational tool in neurosurgical training.

5.6 Analysis Based on Performance

We observed curious dissimilitude in the levels of accuracy achieved by groups of different medical students and different surgeons. Although our sample of surgeons is small, we present a preliminary analysis of surgeons' performance based on their level of experience. In this section, we evaluated a range of metrics for a comparison of the three distinct groups of medical students, and analyzed an improvement of EVD placement accuracy for a comparison of the two distinct groups of neurosurgeons.

TABLE 4: Comparison between groups of students that achieved different levels of accuracy on AR-assisted trials.

	Groups based on Performance		
Criteria	Best	Intermediate	Worst
Total number of students	13	13	7
Number of year 1 students	7	7	5
Number of year 2−4 students	6	6	2
Average accuracy of AR-assisted EVD (mm)	3.89	11.5	21.3
Average completion time of AR-assisted EVD (s)	368.6	343.4	199.2
Average eye gaze focus on contextual guidance (%)	47.76	39.57	31.48
Positivity rate of survey responses on contextual guidance (%)	84.6	79.5	47.6
Positivity rate of survey responses on physical discomfort (%)	69.2	76.9	100

5.6.1 Medical Students

The *best-performing* group is made up of 13 students whose accuracy on AR-assisted trials was under 7mm (average accuracy: 3.89mm). The *intermediate-performing* group is made up of 13 students whose accuracy on AR-assisted trials was higher than 7mm, but still performed better in AR-assisted trials than in freehand EVD trials (average accuracy: 11.5mm). The *worst-performing* group is made up of 7 students who performed worse in AR-assisted trials than in freehand EVD trials (average accuracy: 21.3mm). These results are summarized in Table 4. We observed multiple notable differences between these groups. First, the groups that achieved better accuracy spent considerably more time on the task: to complete EVD catheter insertion, the best-performing group took 25 seconds more than the intermediate-performing group, and *169 seconds (i.e., 85%) more* than the worst-performing group, on average. Second, eye gaze tracking indicates that the worst-performing group paid less attention to the provided contextual guidance than the other groups. *This may indicate that the average accuracy of AR-assisted surgery can be improved by instructing the participants to be slower and more deliberate in their actions and to focus more on the provided contextual guidance.* However, we also saw a notable difference in the levels of self-reported physical discomfort in visual fatigue among these groups: while 100% of the students in the worst-performing group agreed or strongly agreed that they experienced no discomfort, this was only the case for 69.2% of the best-performing group. The observed link between performance and discomfort calls for further investigation of both qualitative and quantitative metrics of different types of discomfort (e.g., physical, visual) in settings with longer and more complex neurosurgical procedures.

5.6.2 Neurosurgeons

The *improved-performance* group is made up of 2 surgeons whose average accuracy on AR-assisted EVD trials of 3.94mm (standard deviation: 0.25mm) improved from the average accuracy on the freehand EVD trials of 11.2mm (standard deviation: 1.57mm). The *consistent-performance* group is made up of 7 surgeons whose average accuracy on AR-assisted EVD trials (average accuracy: 3.90mm) and average accuracy on freehand EVD trials (average accuracy: 2.44mm) were at similar levels. These

TABLE 5: Comparison between groups of surgeons that achieved different levels of accuracy on AR-assisted trials.

	Groups based on Performance	
Criteria	Improved	Consistent
Total number of surgeons	2	7
Average number of years for neurosurgical experience	2	5.8
Average accuracy of freehand EVD (mm)	11.2 ± 1.57	2.44 ± 1.80
Average accuracy of AR-assisted EVD (mm)	3.94 ± 0.25	3.90 ± 1.69
Average accuracy improvement (%)	64.7	N/A

results are summarized in Table 5. We found that the surgeons in the improved-performance group were novice surgeons with an average of 2 years of neurosurgical experience (vs. an average of 5.8 years in the consistent-performance group). The average accuracy improvement of the improved-performance group was 64.7% which is close to the accuracy improvement achieved by the surgeons in prior studies (vs. 61.5% [31]). This may be due to the low number of EVDs performed by novice surgeons in the early stages of residency. In our study, novice surgeons with less than 2 years of experience have performed less than 20 EVDs. Therefore, since the EVD procedure requires prolonged training to become an expert, novice surgeons can still benefit from AR guidance in learning and improving their EVD placement accuracy. This shows that NeuroLens can be more helpful for novice surgeons than for expert surgeons; however, the small number of neurosurgeons in our sample remains as a limitation.

6 Discussion and Future Work

In our user study, we asked the participants to perform the freehand EVD trial first, followed by the AR-assisted EVD trial. In the freehand EVD trial, participants needed to focus on learning how to estimate the target point of the foramen of Monro with anatomical landmarks and a limited FoV. However, since the visualization of the target point was provided to the participants during the AR-assisted EVD trial, they instead focused on other techniques such as the handling of the catheter and the use of AR guidance. Furthermore, participants were not informed about their EVD placement accuracy results and did not learn based on the feedback on their performance. Hence, we believe that this did not contribute to a significant learning effect in our user study design. In future work, we will recruit more participants to formulate one group for performing only the freehand EVD trials and another group for performing only the AR-assisted EVD trials to compare the results between the two groups.

Furthermore, the limitations in tracking bendable EVD catheters and providing limited guidance about catheter trajectory call for future work to improve the system design in NeuroLens. Currently, our system relies on optical marker-based tracking of the EVD catheter to integrate contextual guidance in visualizing the angle, distance to the target, and projection of catheter trajectory. However, our current approach assumes that the inner stylet (which surgeons insert inside the catheter) does not bend; when it does, our system provides incorrect guidance to the surgeons. To address this, we plan to embed sensors such as strain gauges [32] or use a computer vision algorithm [55] to accurately capture the shape of the inner stylet to further improve the accuracy of our AR-based guidance. Moreover, we have designed NeuroLens to provide contextual guidance only in catheter placement; however, EVD placement entails the whole process of identifying external landmarks, drilling Kocher's points (i.e., craniostomy), and determining the catheter trajectory. We will expand our contextual guidance by identifying external landmarks such as the medial canthus and the tragus [20], [30] in real-time using AR by integrating OpenCV with HoloLens 2 to guide surgeons in the planning of drilling Kocher's points at optimal locations [3].

From the prior work to our study, the AR guidance in EVD has only been evaluated for a standard, undisturbed ventricular anatomy. In EVD, anatomical landmarks including the tragus and medial canthus define a catheter trajectory that provides a satisfactory estimate for the standard catheter placement. However, the pathology that involves a tumor or a hemorrhage-producing ventricular entrapment and elevated intracranial pressure causes a mass effect on the ventricular system and displaces this target. In these cases, the surgeons will need to estimate the necessary adjustments to the angle of the trajectory based on an evaluation of the CT scans. In our future work, we will incorporate anomalous ventricular anatomy to further demonstrate the utility of NeuroLens for "single-attempt" EVD placement which will minimize procedure-associated morbidity involved with these more challenging EVD placement scenarios.

Lastly, we have evaluated NeuroLens for training medical students to improve catheter placement accuracy with a future goal of clinical implementation; however, the current NeuroLens setup in a clinical setting has limitations in 1) space constraints due to the external camera setup taking too much space, 2) time constraints due to manual image segmentation [44], [63], and 3) robustness of real-time registration due to occlusion or loss of markers [8], [63]. To address the space constraint, we plan to mount the OptiTrack cameras on the ceiling to declutter the surgical area [15], [25]. To reduce the preparation time, we are currently developing a pipeline for automatically segmenting brain ventricles from the CT scans and visualizing the hologram in the AR headset without user intervention. By computing the automatic image segmentation on the edge server and sending the results to HoloLens 2, our system can visualize the patient-specific ventricular hologram with a shorter preparation time (around 3 min). Finally, we will use OptiTrack's Motion Capture suit [39] to develop a more robust marker model that can tolerate the occlusion of markers in specific scenarios.

7 Conclusion

This paper presents NeuroLens, the first AR-based contextual guidance system that guides neurosurgeons in the catheter placement of the EVD procedure. NeuroLens provides both the anatomical visualization of the patient's ventricular hologram and the guidance on catheter placement, enabled by tracking the catheter. Our evaluations of

NeuroLens with 33 medical students and 9 neurosurgeons, who used NeuroLens to insert an EVD catheter used in clinical settings into a realistic phantom model of a human head, demonstrated that NeuroLens helped students place the catheter closer to its target during the EVD training. Furthermore, our study demonstrated that participants who focused more on the provided guidance achieved higher accuracy. In future work, we will develop approaches to EVD catheter tracking that take the catheter's non-rigidity into account, and will design, develop, and evaluate a wide range of additional contextual guidance for the surgeons.

ACKNOWLEDGMENT

We thank all participants in our user study. We also thank Ritvik Janamsetty and Neha Vutakuri for their work in this project. This work was supported in part by NSF grants CNS-2112562 and CNS-1908051, NSF CAREER Award IIS-2046072, by a Thomas Lord Educational Innovation Grant, and by an AANS Neurosurgery Technology Development Grant.

REFERENCES

[1] Y. Adagolodjo, N. Golse, E. Vibert, M. De Mathelin, S. Cotin, and H. Courtecuisse. Marker-based registration for large deformations-application to open liver surgery. In *Proc. IEEE ICRA*, 2018.

[2] A. AlAzri, K. Mok, J. Chankowsky, M. Mullah, and J. Marcoux. Placement accuracy of external ventricular drain when comparing freehand insertion to neuronavigation guidance in severe traumatic brain injury. *Acta Neurochirurgica*, 159(8):1399–1411, 2017.

[3] M. O. Alves and D. O. Dantas. Mobile augmented reality for craniotomy planning. In *Proc. IEEE ISCC*, 2021.

[4] A. Amini, Y. Zeller, K.-P. Stein, K. Hartmann, T. Wartmann, C. Wex, E. Mirzaee, V. M. Swiatek, S. Saalfeld, A. Haghikia, et al. Overcoming barriers in neurosurgical education: A novel approach to practical ventriculostomy simulation. *Operative Neurosurgery*, pp. 10–1227, 2022.

[5] C. M. Andrews, A. B. Henry, I. M. Soriano, M. K. Southworth, and J. R. Silva. Registration techniques for clinical applications of three-dimensional augmented reality devices. *IEEE Journal of Translational Engineering in Health and Medicine*, 9:1–14, 2020.

[6] M. Birlo, P. E. Edwards, M. Clarkson, and D. Stoyanov. Utility of optical see-through head mounted displays in augmented reality-assisted surgery: A systematic review. *Medical Image Analysis*, 77:102361, 2022.

[7] L. Chen, T. W. Day, W. Tang, and N. W. John. Recent developments and future challenges in medical mixed reality. In *Proc. IEEE ISMAR*, 2017.

[8] S. Chidambaram, V. Stifano, M. Demetres, M. Teyssandier, M. C. Palumbo, A. Redaelli, A. Olivi, M. L. Apuzzo, and S. C. Pannullo. Applications of augmented reality in the neurosurgical operating room: a systematic review of the literature. *Journal of Clinical Neuroscience*, 91:43–61, 2021.

[9] Y.-S. Dho, S. J. Park, H. Choi, Y. Kim, H. C. Moon, K. M. Kim, H. Kang, E. J. Lee, M.-S. Kim, J. W. Kim, et al. Development of an inside-out augmented reality technique for neurosurgical navigation. *Neurosurgical Focus*, 51(2):E21, 2021.

[10] M. Doughty, K. Singh, and N. R. Ghugre. SurgeonAssist-Net: towards context-aware head-mounted display-based augmented reality for surgical guidance. In *International Conference on Medical Image Computing and Computer-Assisted Intervention*. Springer, 2021.

[11] S. Eom, S. Kim, S. Rahimpour, and M. Gorlatova. AR-assisted surgical guidance system for ventriculostomy. In *Proc. IEEE VR Workshops*, 2022.

[12] S. Eom, D. Sykes, S. Rahimpour, and M. Gorlatova. Neurolens: Augmented reality-based contextual guidance through surgical tool tracking in neurosurgery. In *Proc. IEEE ISMAR*, 2022.

[13] T. Fick, J. van Doormaal, E. Hoving, L. Regli, and T. van Doormaal. Holographic patient tracking after bed movement for augmented reality neuronavigation using a head-mounted display. *Acta Neurochirurgica*, 163(4):879–884, 2021.

[14] T. Frantz, B. Jansen, J. Duerinck, and J. Vandemeulebroucke. Augmenting Microsoft's HoloLens with Vuforia tracking for neuronavigation. *Healthcare Technology Letters*, 5(5):221–225, 2018.

[15] D. Gasques, J. G. Johnson, T. Sharkey, Y. Feng, R. Wang, Z. R. Xu, E. Zavala, Y. Zhang, W. Xie, X. Zhang, et al. ARTEMIS: A collaborative mixed-reality system for immersive surgical telementoring. In *Proc. ACM CHI*, 2021.

[16] U. C. Gautam, Y. S. Pydi, S. Selladurai, C. J. Das, A. K. Thittai, S. Roy, and N. V. Datla. A poly-vinyl alcohol (pva)-based phantom and training tool for use in simulated transrectal ultrasound (trus) guided prostate needle biopsy procedures. *Medical Engineering & Physics*, 96:46–52, 2021.

[17] M. S. Greenberg and N. Arredondo. *Handbook of Neurosurgery*, vol. 87. Thieme New York, 2001.

[18] C. Gsaxner, J. Li, A. Pepe, Y. Jin, J. Kleesiek, D. Schmalstieg, and J. Egger. The hololens in medicine: A systematic review and taxonomy. *Medical Image Analysis*, p. 102757, 2023.

[19] C. Gsaxner, J. Li, A. Pepe, D. Schmalstieg, and J. Egger. Inside-out instrument tracking for surgical navigation in augmented reality. In *Proc. ACM VRST*, 2021.

[20] C. Gsaxner, A. Pepe, J. Wallner, D. Schmalstieg, and J. Egger. Markerless image-to-face registration for untethered augmented reality in head and neck surgery. In *International Conference on Medical Image Computing and Computer-Assisted Intervention*. Springer, 2019.

[21] D. Guha, N. M. Alotaibi, N. Nguyen, S. Gupta, C. McFaul, and V. X. Yang. Augmented reality in neurosurgery: a review of current concepts and emerging applications. *Canadian Journal of Neurological Sciences*, 44(3):235–245, 2017.

[22] J. Haemmerli, A. Davidovic, T. R. Meling, L. Chavaz, K. Schaller, and P. Bijlenga. Evaluation of the precision of operative augmented reality compared to standard neuronavigation using a 3D-printed skull. *Neurosurgical Focus*, 50(1):E17, 2021.

[23] R. Hussain, C. Guigou, K. B. Girum, A. Lalande, and A. B. Grayeli. 3D landmark detection for augmented reality based otologic procedures. In *Surgetica*, 2019.

[24] R. Hussain, A. Lalande, C. Guigou, and A. Bozorg-Grayeli. Contribution of augmented reality to minimally invasive computer-assisted cranial base surgery. *IEEE Journal of Biomedical and Health Informatics*, 24(7):2093–2106, 2019.

[25] M. Kanegae, J. Morita, S. Shimamura, Y. Uema, M. Takahashi, M. Inami, T. Hayashida, and M. Sugimoto. Registration and projection method of tumor region projection for breast cancer surgery. In *Proc. IEEE VR*, 2015.

[26] D. Katić, P. Spengler, S. Bodenstedt, G. Castrillon-Oberndorfer, R. Seeberger, J. Hoffmann, R. Dillmann, and S. Speidel. A system for context-aware intraoperative augmented reality in dental implant surgery. *International Journal of Computer Assisted Radiology and Surgery*, 10(1):101–108, 2015.

[27] M. Lai, S. Skyrman, F. Kor, R. Homan, V. G. El-Hajj, D. Babic, E. Edström, A. Elmi-Terander, B. H. Hendriks, and P. H. de With. Development of a ct-compatible, anthropomorphic skull and brain phantom for neurosurgical planning, training, and simulation. *Bioengineering*, 9(10):537, 2022.

[28] M. Lai, S. Skyrman, C. Shan, D. Babic, R. Homan, E. Edström, O. Persson, G. Burström, A. Elmi-Terander, B. H. Hendriks, et al. Fusion of augmented reality imaging with the endoscopic view for endonasal skull base surgery; a novel application for surgical navigation based on intraoperative cone beam computed tomography and optical tracking. *Plos one*, 15(1):e0227312, 2020.

[29] É. Léger, S. Drouin, D. L. Collins, T. Popa, and M. Kersten-Oertel. Quantifying attention shifts in augmented reality image-guided neurosurgery. *Healthcare technology letters*, 4(5):188–192, 2017.

[30] C. Leuze, S. Sathyanarayana, B. L. Daniel, and J. A. McNab. Landmark-based mixed-reality perceptual alignment of medical imaging data and accuracy validation in living subjects. In *Proc. IEEE ISMAR*, 2020.

[31] Y. Li, X. Chen, N. Wang, W. Zhang, D. Li, L. Zhang, X. Qu, W. Cheng, Y. Xu, W. Chen, et al. A wearable mixed-reality holographic computer for guiding external ventricular drain insertion at the bedside. *Journal of Neurosurgery*, 131(5):1599–1606, 2018.

[32] M. A. Lin, A. F. Siu, J. H. Bae, M. R. Cutkosky, and B. L. Daniel. HoloNeedle: augmented reality guidance system for needle placement investigating the advantages of three-dimensional

needle shape reconstruction. *IEEE Robotics and Automation Letters*, 3(4):4156–4162, 2018.
[33] S. Lu, Y. P. Sanchez Perdomo, X. Jiang, and B. Zheng. Integrating eye-tracking to augmented reality system for surgical training. *Journal of Medical Systems*, 44(11):1–7, 2020.
[34] A. J. Lungu, W. Swinkels, L. Claesen, P. Tu, J. Egger, and X. Chen. A review on the applications of virtual reality, augmented reality and mixed reality in surgical simulation: an extension to different kinds of surgery. *Expert review of medical devices*, 18(1):47–62, 2021.
[35] L. Ma, Z. Zhao, B. Zhang, W. Jiang, L. Fu, X. Zhang, and H. Liao. Three-dimensional augmented reality surgical navigation with hybrid optical and electromagnetic tracking for distal intramedullary nail interlocking. *The International Journal of Medical Robotics and Computer Assisted Surgery*, 14(4):e1909, 2018.
[36] E. C. Mackle, J. Shapey, E. Maneas, S. R. Saeed, R. Bradford, S. Ourselin, T. Vercauteren, and A. E. Desjardins. Patient-specific polyvinyl alcohol phantom fabrication with ultrasound and X-ray contrast for brain tumor surgery planning. *Journal of Visualized Experiments*, (161):e61344, 2020.
[37] A. Meola, F. Cutolo, M. Carbone, F. Cagnazzo, M. Ferrari, and V. Ferrari. Augmented reality in neurosurgery: a systematic review. *Neurosurgical Review*, 40(4):537–548, 2017.
[38] R. Muralidharan. External ventricular drains: Management and complications. *Surgical Neurology International*, 6(Suppl 6):S271, 2015.
[39] NaturalPoint. OptiTrack – motion capture suits. https://optitrack.com/ accessories/wear/, 2022.
[40] H. Ofoma, B. Cheaney II, N. J. Brown, B. V. Lien, A. S. Himstead, E. H. Choi, S. Cohn, J. K. Campos, and M. Y. Oh. Updates on techniques and technology to optimize external ventricular drain placement: A review of the literature. *Clinical Neurology and Neurosurgery*, 213:107126, 2022.
[41] B. R. O'Neill, D. A. Velez, E. E. Braxton, D. Whiting, and M. Y. Oh. A survey of ventriculostomy and intracranial pressure monitor placement practices. *Surgical Neurology*, 70(3):268–273, 2008.
[42] A. Pepe, G. F. Trotta, P. Mohr-Ziak, C. Gsaxner, J. Wallner, V. Bevilacqua, and J. Egger. A marker-less registration approach for mixed reality–aided maxillofacial surgery: a pilot evaluation. *Journal of digital imaging*, 32(6):1008–1018, 2019.
[43] M. Pishjoo, K. Khatibi, H. Etemadrezaie, S. Zabihyan, B. Ganjeifar, M. Safdari, and H. Baharvahdat. Determinants of accuracy of freehand external ventricular drain placement by neurosurgical trainees. *Acta Neurochirurgica*, 163(4):1113–1119, 2021.
[44] Z. Qi, Y. Li, X. Xu, J. Zhang, F. Li, Z. Gan, R. Xiong, Q. Wang, S. Zhang, and X. Chen. Holographic mixed-reality neuronavigation with a head-mounted device: technical feasibility and clinical application. *Neurosurgical Focus*, 51(2):E22, 2021.
[45] L. Qian, A. Deguet, Z. Wang, Y.-H. Liu, and P. Kazanzides. Augmented reality assisted instrument insertion and tool manipulation for the first assistant in robotic surgery. In *Proc. IEEE ICRA*, 2019.
[46] N. Rewkowski, A. State, and H. Fuchs. Small marker tracking with low-cost, unsynchronized, movable consumer cameras for augmented reality surgical training. In *Proc. IEEE ISMAR-Adjunct*, 2020.
[47] M. Schneider, C. Kunz, A. Pal'a, C. R. Wirtz, F. Mathis-Ullrich, and M. Hlaváč. Augmented reality–assisted ventriculostomy. *Neurosurgical Focus*, 50(1):E16, 2021.
[48] W. Si, X. Liao, Q. Wang, and P.-A. Heng. Augmented reality-based personalized virtual operative anatomy for neurosurgical guidance and training. In *Proc. IEEE VR*, 2018.
[49] S. Skyrman, M. Lai, E. Edström, G. Burström, P. Förander, R. Homan, F. Kor, R. Holthuizen, B. H. Hendriks, O. Persson, et al. Augmented reality navigation for cranial biopsy and external ventricular drain insertion. *Neurosurgical Focus*, 51(2):E7, 2021.
[50] SMiF. High resolution X-ray computed tomography scanner. https://smif.pratt.duke.edu/node/153, 2022.
[51] T. Song, C. Yang, O. Dianat, and E. Azimi. Endodontic guided treatment using augmented reality on a head-mounted display system. *Healthcare Technology Letters*, 5(5):201–207, 2018.
[52] C. Steiert, S. P. Behringer, L. M. Kraus, M. Bissolo, T. Demerath, J. Beck, J. Grauvogel, and P. C. Reinacher. Augmented reality–assisted craniofacial reconstruction in skull base lesions—an innovative technique for single-step resection and cranioplasty in neurosurgery. *Neurosurgical Review*, pp. 1–11, 2022.
[53] M. Stuart, J. Antony, T. Withers, and W. Ng. Systematic review and meta-analysis of external ventricular drain placement accuracy and narrative review of guidance devices. *Journal of Clinical Neuroscience*, 94:140–151, 2021.
[54] H. Suenaga, H. H. Tran, H. Liao, K. Masamune, T. Dohi, K. Hoshi, and T. Takato. Vision-based markerless registration using stereo vision and an augmented reality surgical navigation system: a pilot study. *BMC medical imaging*, 15(1):1–11, 2015.
[55] X. Sun, S. B. Murthi, G. Schwartzbauer, and A. Varshney. High-precision 5DoF tracking and visualization of catheter placement in EVD of the brain using AR. *ACM Transactions on Computing for Healthcare*, 1(2):1–18, 2020.
[56] R. Tang, L.-F. Ma, Z.-X. Rong, M.-D. Li, J.-P. Zeng, X.-D. Wang, H.-E. Liao, and J.-H. Dong. Augmented reality technology for preoperative planning and intraoperative navigation during hepatobiliary surgery: a review of current methods. *Hepatobiliary & Pancreatic Diseases International*, 17(2):101–112, 2018.
[57] P. Tu, Y. Gao, A. J. Lungu, D. Li, H. Wang, and X. Chen. Augmented reality based navigation for distal interlocking of intramedullary nails utilizing Microsoft HoloLens 2. *Computers in Biology and Medicine*, 133:104402, 2021.
[58] F. Van Gestel, T. Frantz, C. Vannerom, A. Verhellen, A. G. Gallagher, S. A. Elprama, A. Jacobs, R. Buyl, M. Bruneau, B. Jansen, et al. The effect of augmented reality on the accuracy and learning curve of external ventricular drain placement. *Neurosurgical Focus*, 51(2):E8, 2021.
[59] N. Weibel, D. Gasques, J. Johnson, T. Sharkey, Z. R. Xu, X. Zhang, E. Zavala, M. Yip, and K. Davis. ARTEMIS: mixed-reality environment for immersive surgical telementoring. In *Proc. ACM CHI Extended Abstracts*, 2020.
[60] P. Weinstock, R. Rehder, S. P. Prabhu, P. W. Forbes, C. J. Roussin, and A. R. Cohen. Creation of a novel simulator for minimally invasive neurosurgery: fusion of 3d printing and special effects. *Journal of Neurosurgery: Pediatrics*, 20(1):1–9, 2017.
[61] J. Woodward and J. Ruiz. Analytic review of using augmented reality for situational awareness. *IEEE Transactions on Visualization and Computer Graphics*, 2022.
[62] D. S. Yanni, B. M. Ozgur, R. G. Louis, Y. Shekhtman, R. R. Iyer, V. Boddapati, A. Iyer, P. D. Patel, R. Jani, M. Cummock, et al. Real-time navigation guidance with intraoperative CT imaging for pedicle screw placement using an augmented reality head-mounted display: A proof-of-concept study. *Neurosurgical Focus*, 51(2):E11, 2021.
[63] G. Yavas, K. E. Caliskan, and M. S. Cagli. Three-dimensional–printed marker–based augmented reality neuronavigation: a new neuronavigation technique. *Neurosurgical Focus*, 51(2):E20, 2021.
[64] F. Zhang, L. Chen, W. Miao, and L. Sun. Research on accuracy of augmented reality surgical navigation system based on multi-view virtual and real registration technology. *IEEE Access*, 8:122511–122528, 2020.
[65] L. Zhang, I. Kamaly, P. Luthra, and P. Whitfield. Simulation in neurosurgical training: a blueprint and national approach to implementation for initial years trainees. *British Journal of Neurosurgery*, 30(5):577–581, 2016.
[66] S. Zhao, X. Xiao, Q. Wang, X. Zhang, W. Li, L. Soghier, and J. Hahn. An intelligent augmented reality training framework for neonatal endotracheal intubation. In *Proc. IEEE ISMAR*, 2020.
[67] J.-H. Zhu, R. Yang, Y.-X. Guo, J. Wang, X.-J. Liu, and C.-B. Guo. Navigation-guided core needle biopsy for skull base and parapharyngeal lesions: a five-year experience. *International Journal of Oral and Maxillofacial Surgery*, 50(1):7–13, 2021.

Sangjun Eom (Graduate Student Member, IEEE) received the B.S. (with distinction), in 2017, and M.S. degrees in Electrical Engineering Technology from Purdue University, West Lafayette, IN, USA, in 2020. She is currently pursuing a Ph.D. degree in Electrical and Computer Engineering at Duke University, NC, USA. Her current research interests include Augmented Reality and Internet of Things.

Seijung Kim (Student Member, IEEE) is currently pursuing the M.S. degree in Biomedical Engineering at Duke University, Durham, NC, USA. Her research interests are Digital Health and Biomedical Data Science. She earned a B.S. degree in Biomedical Engineering and a B.A. degree in Computer Science at Duke University, Durham, NC, USA.

Joshua Jackson received his B.S in chemical engineering from Tennessee Tech University, Cookeville, TN, USA, Master of Chemical Engineering degree from Auburn University, Auburn, AL and M.D. and Ph.D. degrees from the University of Alabama at Birmingham, Birmingham, AL, USA. He is currently a resident in the neurosurgery program at Duke University, Durham, NC, USA. His specific interests are in brain tumor immunotherapy for which he was awarded an R25 NIH training grant. He maintains engineering interests in medical device development and clinical translation.

David Sykes received his bachelor's degree in biochemistry and molecular biology at Washington University in St. Louis, MO, USA, where he graduated with honors in 2020. At Washington University, he performed research on bone metabolism, a topic in which he is published. After graduation, he enrolled at the Duke University School of Medicine, Durham, NC, USA, where he plans to graduate with his M.D. in 2024. His research interests include emerging technologies, minimally invasive spine surgery, wide-awake spine surgery, and cerebrovascular disease. He intends to pursue a career in neurosurgery after graduation in 2024.

Shervin Rahimpour is a neurosurgeon at the University of Utah and director of functional neurosurgery. He specializes in the surgical treatment of epilepsy, movement disorders and pain. He obtained his undergraduate degree from the University of Colorado in Mathematics and Biochemistry. He obtained his medical degree from the University of Colorado and went on to Duke University for neurosurgical training where he also completed subspecialty fellowship training in functional neurosurgery. His research interests are in intra-operative electrophysiology and testing with a primary goal of improving the understanding of how neurodegenerative disorders effect brain function in terms of brain activity and oscillations and how neuromodulation may alleviate these pathologic circuits. His lab also dedicates efforts towards innovation in functional neurosurgery to improve the care of patients undergoing surgery for movement disorders, epilepsy and pain. This includes prospective patient registries, leveraging mixed/virtual reality for patient education and surgical training and developing novel surgical tools.

Maria Gorlatova (S'11, GS'12, M'15) received the B.Sc. (summa cum laude) and M.Sc. degrees in electrical engineering from the University of Ottawa, Ottawa, ON, Canada, and the Ph.D. degree in electrical engineering from Columbia University, New York, NY, USA. She is an Assistant Professor of Electrical and Computer Engineering and Computer Science with Duke University, Durham, NC, USA. She has several years of industry experience, and has been affiliated with Telcordia Technologies, Piscataway, NJ, USA, IBM, Armonk, NY, USA, and D. E. Shaw Research, New York, NY, USA. Her current research interests include architectures, algorithms, and protocols for emerging pervasive technologies. Dr. Gorlatova was a recipient of the Google Anita Borg USA Fellowship, the Canadian Graduate Scholar NSERC Fellowships, and the Columbia University Presidential Fellowship. She was a co-recipient of the 2011 ACMSenSys Best Student Demonstration Award, the 2011 IEEE Communications Society Award for Advances in Communications, and the 2016 IEEE Communications Society Young Author Best Paper Award.